Characteristics in hard conformal EHL line contacts

Ferdinand Schmid, Constantin Paschold, Thomas Lohner and Karsten Stahl
Gear Research Center (FZG), Department of Mechanical Engineering, School of Engineering and Design, Technical University of Munich, Munich, Germany

Abstract

Purpose – Internal gearings are commonly used in transmissions due to their advantages like high-power density. To ensure high efficiency, load-carrying capacity and good noise behavior, a profound knowledge of the local gear mesh is essential. The tooth contact of internal gears relates to a convex and concave surface that form a conformal contact. This is in contrast to external gears, where two convex surfaces form a contraformal contact. This paper aims at a better understanding of conformal contacts under elastohydrodynamic lubrication (EHL) to improve the design of internal gearings.

Design/methodology/approach – An existing numerical EHL model is used for studying the characteristic properties of a hard conformal EHL line contact. A hard contraformal EHL line contact is studied as reference. Non-Newtonian fluid behavior and thermal effects are considered. By taking into account the local contact conformity and kinematics, the effects and relevance of the curvature of the lubricant gap and micro-slip are analyzed. In a parameter study, scale effects of the contact radii on film thickness, temperature rise and friction are examined.

Findings – The curvature of the lubricant gap and effects of micro-slip are small in hard conformal EHL line contacts. For high micro-slip, it can be neglected. Hence, the modeling of conformal contacts using an equivalent geometry of the contact problem is reasonable. The parameter study shows beneficial tribological aspects of the conformal contact compared to the contraformal contact. Higher film thickness and lower fluid coefficient of friction are observed for conformal contacts, which can be attributed to lower pressures for the case of the same external normal force, or to a higher contact temperature rise for the case of equivalent contact pressure.

Originality/value – Despite its widespread existence, the local geometry and kinematics in hard conformal EHL line contacts like in internal gearings have been rarely studied. The findings help for a better understanding of local contact characteristics and its relevance. The quantified scale effects help to improve the efficiency and load-carrying capacity of machine elements with hard conformal EHL contacts, like internal gearings.

Peer review – The peer review history for this article is available at: https://publons.com/publon/10.1108/ILT-12-2022-0366/

Keywords Conformal contact, Hard EHL contact, EHL simulation, Line contact, Finite element method (FEM), Micro-slip, Internal gearing

Paper type Research paper

Nomenclature

b_H = Hertzian half width in m;
c_p = Specific heat capacity in J/(kg K);
D = Disk diameter in m;
E = Young's modulus in N/m^2;
F = Functional trajectory of surface/contact;
F_N = Normal load in N;
F_R = Friction force in N;
h_c = Central film thickness in m;
h_m = Minimum film thickness in m;
loc = Level of conformity;
$p(_{x,\ z})$ = Pressure in (x,z direction) in N/m^2;
p_H = Hertzian Pressure in N/m^2;
$R_{1,2}$ = Radius of curvature of body 1,2 in m;
$r_{1,2}$ = Local radius of curvature of body 1,2 in m;
r_x = Local radius of curvature in m;
R_x = Equivalent radius of curvature in m;
s_δ = Micro-slip;
s = Macro-slip;
s_{tot} = Total slip;
t = Thickness in m;
T = Temperature rise in K;

The current issue and full text archive of this journal is available on Emerald Insight at: **https://www.emerald.com/insight/0036-8792.htm**

Industrial Lubrication and Tribology
75/7 (2023) 730–740
Emerald Publishing Limited [ISSN 0036-8792]
[DOI 10.1108/ILT-12-2022-0366]

This paper forms part of a special section "Insights into the work of a new generation of young tribologists", guest edited by Max Marian.

The authors would like to thank for the possibility to contribute to the special issue "Insights into the Work of a New Generation of Young Tribologists" and the support received from the colleagues.

The presented results are based on the research project 03EN4005A; supported by the Federal Ministry for Economic Affairs and Climate Action (BMWK) and supervised by the Project Management Agency Jülich (PtJ). The authors would like to thank for the sponsorship and support received from BMWi and Project Management Agency PtJ.

Received 15 December 2022
Revised 8 March 2023
26 April 2023
Accepted 26 April 2023

$v_{1,2}$ = Surface velocity of solid body 1,2 in m/s;
$v_{1\delta,2\delta}$ = Surface velocity of deformed solid body 1,2 in m/s;
v_g = Sliding velocity in m/s;
v_t = Tangential velocity in m/s;
v_Σ = Sum velocity in m/s;
VI = Viscosity index;
x = Gap length direction in m;
x_s = Global (spatial) length coordinate in m;
X = Gap length direction (dimensionless);
X_s = Global (spatial) length coordinate (dimensionless);
z = Gap height direction in m;
z_s = Global (spatial) height coordinate in m;
Z = Gap height direction (dimensionless); and
Z_s = Global (spatial) height coordinate (dimensionless).

Greek symbols

α = Inclination angle in °;
$\delta_{1,2}$ = Deformation of the equivalent resp. contact body 1,2 in m;
δ_μ = Relative difference of coefficient of friction;
υ = Kinematic viscosity in m^2/s; Poisson's ratio;
λ = Thermal conductivity in W/(m K);
μ = Coefficient of friction;
μ_c = Coefficient of friction of the curved contact;
ρ = Density in kg/m^3;
τ = Shear stress in N/m^2; and
ω = Rotational speed in rad/s.

Indices

1 = Lower solid body;
2 = Upper solid body;
max = Maximum; and
s = Spatial.

1. Introduction

A conformal contact refers generally to a paired convex and concave surface and occurs in many machine elements like pinned joints, bearings, sealings and gearings. The contact pressures, kinematics and degree of conformity can differ substantially.

A conformal contact is often characterized by low to medium contact pressure and high contact area. Booker *et al.* (2010) give an extensive overview about investigations on conformal elastohydrodynamically lubricated (EHL) contacts. Most studies are focused on journal bearings, which are characterized by a very high degree of conformity with relatively low contact pressure in the soft EHL regime (Johnson, 1970). For example, experimental and numerical analyses were performed by Bergmann *et al.* (2018). Fritzson (2018) gives an insight into the modeling of transient conformal thermal EHL contacts concentrating on journal bearings. Fang *et al.* (1999) developed and presented an EHL and traction test-rig for internal line contacts. Napel (1994) addresses aspects of the EHL of contraformal and conformal contacts but does not elaborate differences between both contacts. Jia *et al.* (2019) modeled wear in conformal contacts under mixed EHL conditions for an exemplary pin-on-disk contact. Zhang *et al.* (2020) investigated the influence of contact size, respectively, the equivalent radius of curvature on high conformity contacts between finite bushes and pins in chains. Geometrical conformity can also occur locally, for example when a stiff and compliant material is paired (Maier *et al.*, 2017).

Contrary to lowly loaded lubricated conformal contacts like in journal bearings, the highly loaded lubricated contacts occur for example in rolling bearings between the outer raceway and the rolling elements as well as in internal gearings between the ring and planet gears. The highly loaded lubricated conformal contact in rolling bearings is studied, for example by Schleich (2013). Besides, Schoo (1985) investigated the contact conditions in internal gearings and found lower load-dependent gear power losses compared to external gearings. Investigations on load-dependent gear power losses of internal gearings were also performed by Gevigney *et al.* (2013).

Only few studies exist that elaborate characteristics of the highly loaded conformal contact compared to the contrafomal contact. Fagan and McConnachie (2001) and Blanco-Lorenzo *et al.* (2018) performed numerical studies on the dry conformal contact problem. Johns-Rahnejat *et al.* (2020) investigated the influence of a parabolic pressure distribution in dry conformal contacts considering different conformity levels. The authors show very good agreement between finite element approaches and Hertzian theory, when the level of conformity is small. This is generally the case for conformal gearings (Johns-Rahnejat *et al.*, 2020).

Applying the widely used equivalent body modeling, where the contact problem is reduced into an equivalent contact between a cylinder and a plane (Habchi, 2018), a conformal and contraformal contact only differ in its equivalent radius of curvature. Piccigallo (1996) shows the influence of the equivalent radius of curvature on the coefficient of friction for the case of constant operating conditions. He emphasizes the importance of considering thermal and non-Newtonian effects in modeling EHL contacts. Liu *et al.* (2012) show the importance of the influence of contact temperature when comparing different contact sizes and different radii of curvature, respectively. A decreasing coefficient of friction with increasing radius of curvature is shown. Liu *et al.* (2021) investigated the influence of the radius of curvature on the coefficient of friction for a circular contact using a non-Newtonian and thermal EHL model. They also show a lower coefficient of friction for higher radii of curvature R_x especially when considering thermal properties. Philippon *et al.* (2021) discuss the complexity when comparing friction of different geometry pairings. They confirm a decreasing coefficient of friction with increasing equivalent radius of curvature as well as higher contact temperatures.

Besides the different equivalent radii of curvature, there are local contact characteristics. If a contact consists of two paired rolling elements with different radii of curvature, the contact area is curved (Czichos and Habig, 2015). Therefore, a conformal contact has always a curved contact area. A contraformal contact can also have a curved contact area but has not, if the two rolling elements consist of the same radii. In the case of different radii of curvature there occurs micro-slip in the contact, which is also called Heathcote slip (Heathcote, 1921).

This study considers the conformal EHL line contact as it occurs in internal steel gearings characterized by high pressures of over 1 GPa (Schudy, 2010). Such contact conditions are categorized in the hard EHL regime (Johnson, 1970). Figure 1 shows a comparison between an internal gearing with

Figure 1 Contraformal (a) and conformal (b) gear mesh of an internal and external gearing

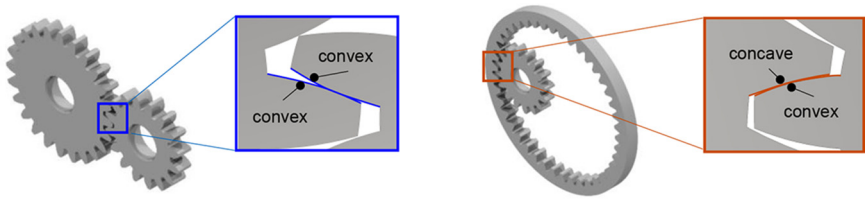

(a) (b)

Source: Created by author

conformal contact and an external gearing with contraformal contact. The characteristics of conformal hard EHL contacts in internal gearings have been rarely addressed in literature, particularly the local geometry and kinematics in the contact. Its effects and its relevance are unclear. Therefore, the local geometry and kinematics as well as scale effects in conformal hard EHL line contacts are analyzed in detail and discussed in comparison to contraformal hard EHL line contacts.

Preliminary results of this study were partly presented at a technical session at the 5th Young Tribological Researcher Symposium of the German Tribology Society in 2022.

2. Methods

In this section, the underlying methods to study the characteristics of conformal hard EHL contacts are described. It is based on representing an internal gear contact by an analogous disk contact. In the following, the object of investigation, operating conditions, investigated parameters, numerical EHL model and material models are described.

2.1 Object of investigation

The object of investigation is a contact between two disks. The contraformal reference setup refers to two disks with external raceways as considered by Hofmann *et al.* (2021). The radii of curvature of the two convex disks are identical with $R_{1,2}$ = 40 mm. The conformal setup refers to a disk with internal raceway and a disk with external raceway, where $R_1 = -125$ mm and R_2 = 40 mm. The geometrical and material properties of the considered disks are shown in Figure 2. The considered bulk material is case-hardened steel (16MnCr5). The material properties are listed in Table 1. The surface contact velocities of the disks are designated with v_1 and v_2. The slip s in the disk contact is defined as:

$$s = \frac{v_1 - v_2}{v_1} \tag{1}$$

The sum velocity v_Σ in the disk contact is defined as:

$$v_\Sigma = v_1 + v_2 \tag{2}$$

The disk contact problem is reduced to an equivalent contact between a disk and plane. The equivalent radius of curvature R_x reads:

$$R_x = \frac{R_1 \cdot R_2}{R_1 + R_2} \tag{3}$$

A disk with internal raceway is considered mathematically by a negative algebraic sign.

2.2 Operating conditions

The disk contacts are considered as fully flooded EHL contact. Ideal smooth surfaces are assumed. The mineral oil MIN100 (ISO VG 100) with $v(40°C)$ = 95 mm^2/s and $v(100°C)$ = 10 mm^2/s is considered. The density is $\rho(15°C)$ = 885 kg/m^3 and the viscosity index is VI = 81.

Figure 2 Considered contraformal (a) and conformal disk (b) contact as main study setup

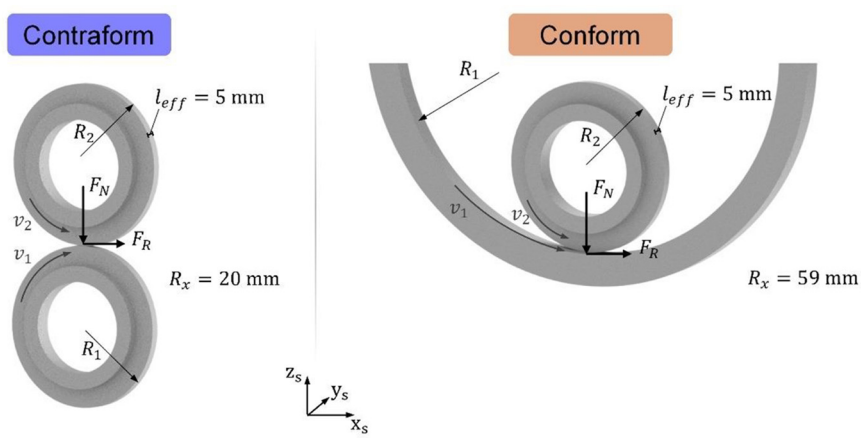

(a) (b)

Source: Created by author

Table 1 Disk material properties

	Contraformal	Conformal	
R_1	40	−125	mm
R_2	40	40	mm
R_x	20	59	Mm
$E_{1,2}$	210	210	GPa
$\nu_{1,2}$	0.3	0.3	
$\rho_{1,2}$	7,760	7,760	kg/m^3
$\lambda_{1,2}$	44	44	$\frac{W}{m \cdot K}$
$c_{p1,2}$	431	431	$\frac{J}{m \cdot K}$

Source: Created by author

A representative gear contact operating condition is defined as reference with a Hertzian pressure of $p_H = 1{,}200\,\mathrm{N/mm^2}$ (normal force of $F_N = 3{,}921\,\mathrm{N}$ for the contraformal disk contact), sum velocity of $v_\Sigma = 8\,\mathrm{m/s}$, slip of $s = 20\%$ and oil inlet and disk bulk temperature of $\vartheta = 90°\mathrm{C}$. The oil kinematic viscosity $v(90°\mathrm{C})$ is $13\,\mathrm{mm^2/s}$ and the density $\rho(90°\mathrm{C})$ is $844\,\mathrm{kg/m^3}$. Regarding load, it is differentiated between equivalent nominal normal force and equivalent Hertzian pressure when comparing the conformal and contraformal disk contact. If not specified, the comparison is based on equivalent Hertzian pressure in the following. For the investigation of local geometry and kinematics, the contact conditions are varied. In particular, for the influence of the curvature in section 3.1, the investigations of the speed and pressure range are extended to $v_\Sigma = 4\ldots16\,\mathrm{m/s}$ and $p_H = 400\ldots1{,}200\,\mathrm{N/mm^2}$. Moreover, for the investigation of micro-slip in section 3.2, low slip values from $s = 0\ldots2\%$ are considered. The influence of the equivalent radius of curvature $R_x = 10\ldots60\,\mathrm{mm}$ is studied in section 3.3 for equivalent nominal normal force and equivalent Hertzian pressure for the reference operating condition.

2.3 Numerical modeling

The numerical EHL model used is based on Lohner *et al.* (2016) and Ziegltrum *et al.* (2017, 2018). A two-dimensional model considering an infinite contact length is applied. The EHL model with all relevant physics is implemented in a commercial multiphysics software and solved based on the finite element method in a full system approach according to Habchi (2018). For modeling the lubricant properties, the formulated models and the corresponding oil data and parameters are adopted from Farrenkopf *et al.* (2022). For description of the temperature dependency of the viscosity, a model according to Vogel (1921), Fulcher (1925) and Tammann and Hesse (1926) is used. To describe the pressure dependency of the viscosity, a model according to Roelands (1966) is referred. Considering non-Newtonian fluid behavior, the Eyring model (Eyring, 1936) is used. The lubricant density is determined by the Bode (1989) model. Thermal behavior is considered with models according to Larsson and Andersson (2000).

As finite element modeling and Hertzian theory show good accordance for small conformity as in conformal gearings (Johns-Rahnejat *et al.*, 2020), the considered disk contacts are transferred to equivalent contact problems. In doing so, the information about the original disk geometries is lost. Therefore, a conformal and contraformal contact can result in the same equivalent contact model. Although the conformal EHL contact area can be curved, the main fluid flow direction is assumed to be one-dimensional (Bartel, 2010). This is possible due to the small relation of lubricant gap height to contact length. This approximation is also widely used for high conformity contacts in journal bearings (Bobach, 2018; Lang and Steinhilper, 1978). The equivalent model is non-dimensionalized to obtain a geometry-independent mesh for simplification of numerical solving (Habchi, 2018). For depiction of local contact geometry from numerical results, the non-dimensionalized contact is dimensionalized again after solving. Then, the equivalent plane-disk model is reshaped into the real two disk geometries.

The coefficient of friction is determined by calculating the integral of the shear stress along the contact in the middle of the lubricant film, in the following designated as centerline $Z = 0.5$; (Habchi, 2018):

$$\mu = \frac{f_{res,x}}{f_N} = \frac{\int_{x_{in}}^{x_{ex}} \tau|_{Z=0.5}(x)\,dx}{f_N} \tag{4}$$

3. Results and discussion

In this section, the local characteristics of the conformal hard EHL disk contact as the local contact geometry and the micro-slip are analyzed. In addition, the influence of the equivalent radius of curvature on the film thickness and coefficient of friction is evaluated.

3.1 Local contact conformity

For contacting rolling elements with different radii of curvature, the centerline of the contact area is curved (Czichos and Habig, 2015). Therefore, a hard conformal EHL contact is always curved. Figure 3 shows the calculated lubricant gap profiles for the considered conformal and contraformal disk contact for $F_N = 3921\,\mathrm{N}$, $v_\Sigma = 8\,\mathrm{m/s}$, $s = 20\%$ and $\vartheta = 90°\mathrm{C}$. For visualization purposes, it is shown non-dimensionalized in Figure 3 (a) and (b) as well as dimensionalized in Figure 3 (c) and (d). As the contraformal EHL contact in Figure 3 (c) results from two disks with equivalent radius ($R_1 = R_2$), the centerline of the lubricant gap is straight. Contrary, for the conformal EHL contact in Figure 3 (d), the centerline is curved. Note that the dimensions in the gap height direction are much smaller than in gap length direction.

The local conformity of an EHL contact can be quantified. It is mathematically described by the local radius of curvature r_x. In general, a local radius of a functional curve f is described by:

$$r_x(x_s) = \left| \frac{\left[1 + \left(\frac{\partial f(x_s)}{\partial x_s}\right)^2\right]^{\frac{3}{2}}}{\left(\frac{\partial^2 f(x_s)}{\partial x_s^2}\right)} \right|, \tag{5}$$

where the curves for the surfaces are obtained by:

$$f(x_s) = \frac{x_s^2}{2 \cdot R_{1,2}} \pm \delta_{1,2}. \tag{6}$$

Based on Figure 3, the local radius of curvature r_x of the deformed surfaces of the contraformal and conformal EHL

Figure 3 Lubricant gap curvature of the conformal (a) and contraformal (b) disk contact in nondimensional (a),(b) and dimensional form (c),(d) for F_N = 3,921 N, v_Σ = 8 m/s, s = 20% and ϑ = 90°C

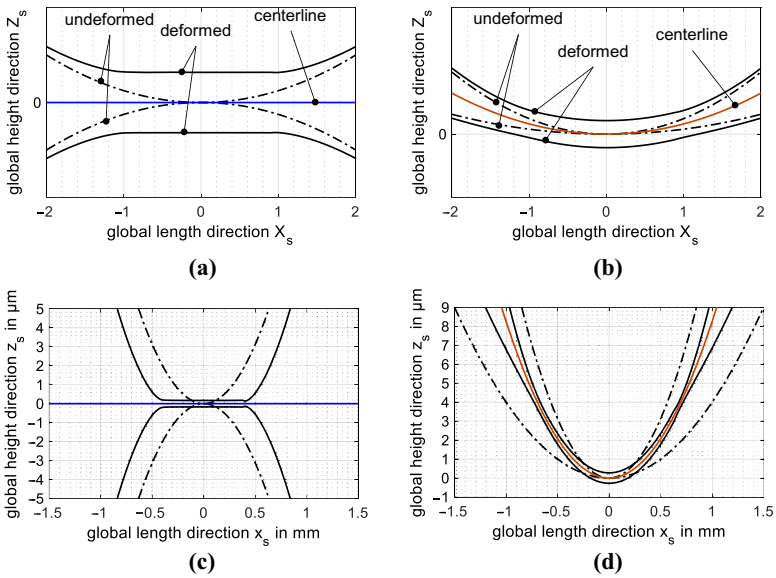

Source: Created by author

contact is shown in Figure 4 (a) and (b). In the inlet and outlet zone of the EHL contact, r_x increases for the convex surface and decreases for the concave surface. In the contact zone, both surfaces show nearly identical values of r_x, forming a parallel but curved lubricant gap. Outside the deformed contact zone, r_x corresponds to the macroscopic radius of curvature.

The radius of curvature r_x of the centerline can be approximated by equation (7) according to Heathcote (1921). Results show accordance with the findings in Figure 4:

$$r_x = 2 \cdot \left(\frac{1}{R_1} - \frac{1}{R_2} \right)^{-1}. \tag{7}$$

Besides the local contact radius of curvature, the inclination angle α can be evaluated. It is defined as the angle between the centerline of the EHL contact and a horizontal line representing the global contact length direction. The inclination angle α can be calculated as:

$$\alpha = tan^{-1}\left(\frac{\partial(f)}{\partial x_s} \right). \tag{8}$$

The maximum inclination of conformal contacts lies in the begin and the end of contact. The higher the conformity, the larger the contact area and therefore the inclination angle α.

As a consequence of contact inclination, the pressure distribution in conformal contacts is also "curved." Figure 5 shows the pressure distribution for the considered contraformal and conformal EHL contact. While the pressure distribution of the contraformal contact only contains pressure components in the global height direction z_s, the conformal contact has additional pressure components in the global x_s direction.

Figure 4 Local radius of curvature of the contraformal (a) and conformal (b) disk contact along gap length direction for F_N = 3,921 N, v_Σ = 8 m/s, s = 20% and ϑ = 90°C

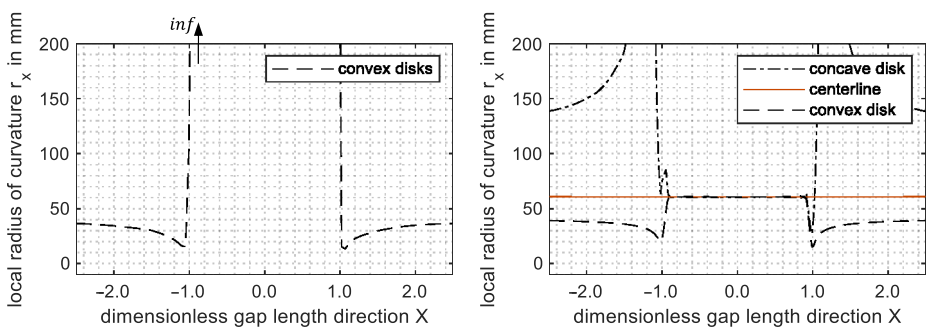

Source: Created by author

Figure 5 Pressure distribution of the contraformal (a) and conformal (b) disk contact along gap length direction for p_H = 1,200 N/mm^2 and s = 20%, v_Σ = 8 m/s, ϑ = 90°C

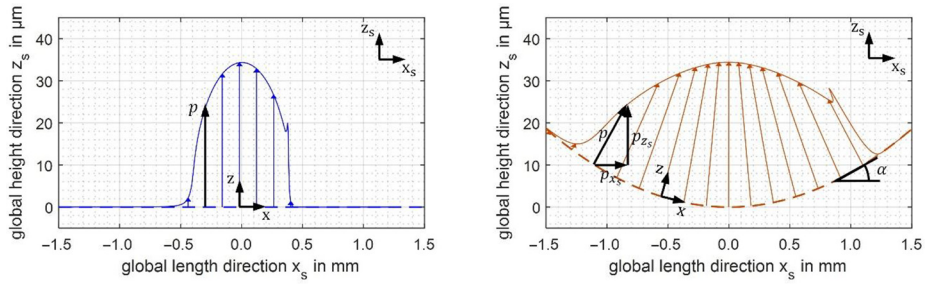

(a) **(b)**

Source: Created by author

The pressure components in the global x_s direction can be calculated as:

$$p_{x_s} = -p \cdot sin(\alpha). \tag{9}$$

In analogy, the shear stress component in global x_s direction can be evaluated by:

$$\tau_{x_s} = \tau \cdot cos(\alpha). \tag{10}$$

In a static dry contact, the pressure distribution is symmetric along the gap length direction. The pressure distribution in an EHL contact is generally not symmetric due to the inlet zone and constriction in the outlet zone (see Figure 5). When integrating the pressure distribution of a conformal EHL contact, a force perpendicular to the normal force acts resulting in a friction force. Based on equation (4), the coefficient of friction of a conformal EHL contact $\boldsymbol{\mu}_c$ results from the shear stress and pressure in global x_s direction:

$$\mu_c = \frac{\int_{x_{in}}^{x_{ex}} \tau_{x_s}|_{Z=0.5}(x)\, dx_s}{f_N} + \frac{\int_{x_{in}}^{x_{ex}} p_{x_s}(x)\, dx_s}{f_N}. \tag{11}$$

To evaluate the deviation between the individual evaluation methods of the coefficient of friction given in equation (4) and (11), the relative difference of coefficient of friction δ_μ is calculated by:

$$\delta_\mu = \frac{\mu_c - \mu}{\mu}. \tag{12}$$

Figure 6 shows the relative difference δ_μ between the coefficient of friction evaluated as in equation (4) and the coefficient of friction evaluated as in equation (11) for various boundary conditions. For low friction, the pressure term in equation (11) dominates leading to high values of δ_μ. This is mainly due to the asymmetric pressure distribution. Figure 6 shows especially for low Hertzian pressures, high sum velocities and low slip values higher values of δ_μ of up to 7%. However, for high pressures the deviation δ_μ is less than 1%. It should be noted that the evaluation of the coefficient of friction in the contact centerline is not necessarily sufficient for a holistic consideration of friction, because the resulting force of a contact body emerges of the overall integrated pressure and shear stresses at the body surfaces.

Figure 6 Relative difference of the coefficient of friction due to the curvature of the conformal EHL contact for various operating conditions with ϑ = 90°C

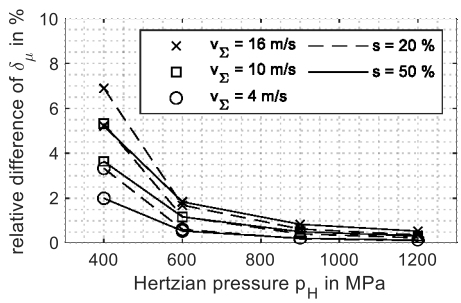

Source: Created by author

3.2 Local contact kinematics

A conformal contact induces additional micro-slip inside the contact, because of different radii of curvature (Czichos and Habig, 2015). Figure 7 shows schematically the kinematics of the considered contraformal and conformal disk contact. The surface velocity around the center of rotation is superimposed by the deformation in the contact resulting in a deviation from the undeformed surface velocity. The concave disk is impinged by an additional incremental velocity Δv, whereas the surface velocity of the convex disk is reduced in the deformed state.

The surface velocities $v_{1\delta}$ and $v_{2\delta}$ in the contact considering the deformation of the surfaces can be approximated by:

$$v_{1\delta,2\delta} = |\omega_{1,2}| \cdot \left(|R_{1,2}| - \frac{|R_{1,2}|}{R_{1,2}} \cdot |\delta_{1,2}| \right). \tag{13}$$

For the considered disk contacts, the total slip s_{tot} is then composed of the macro-slip s as well as the micro-slip s_δ and can be written as:

$$\begin{aligned} s_{tot} &= \frac{v_1\left(1 - \frac{|\delta_1|}{R_1}\right) - v_2\left(1 - \frac{|\delta_2|}{R_2}\right)}{v_1} \\ &= \underbrace{\frac{(v_1 - v_2)}{v_1}}_{macro-slip\ s} + \underbrace{\frac{-v_1 \frac{|\delta_1|}{R_1} + v_2 \frac{|\delta_2|}{R_2}}{v_1}}_{macro-slip\ s_\delta}. \end{aligned} \tag{14}$$

Figure 7 Schematic kinematics of the contraformal (a) and conformal (b) disk contact along gap length direction with the formation of the micro-slip

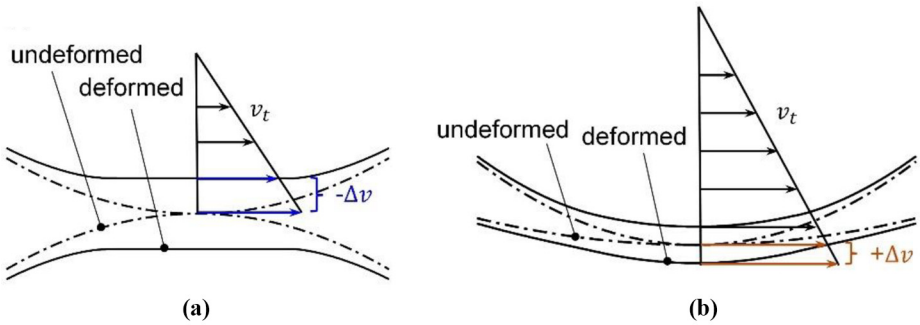

Source: Created by author

For evaluating the relevance of the micro-slip in the considered contraformal and conformal EHL contacts, the following relation is used:

$$\frac{s_\delta}{s} = \frac{-\frac{|\delta_1|}{R_1} v_1 + \frac{|\delta_2|}{R_2} v_2}{v_1 - v_2}. \tag{15}$$

Figure 8 shows the evaluated micro-slip ratio for the reference-operating condition (section 2.2) in the contact along the gap length direction. For both disk contacts, the additional micro-slip is a function of the gap length coordinate, which is due the coupling with the surface deformation. Although the considered contraformal hard EHL contact consists of two disks with equivalent radius of curvature ($R_1 = R_2$), the micro-slip is not zero. This can be understood by equation (14). The micro-slip in the contraformal contact only vanishes for the case of pure rolling ($v_1 = v_2$). Moreover, the micro-slip is negative. Hence, the total slip in the contact is smaller than the nominal imposed macro-slip. Contrary, for the conformal contact the value of the macro-slip is higher compared to the contraformal contact and further positive. Therefore, the micro-slip in the conformal contact adds to the macro-slip, resulting in higher total slip inside the contact. However, the additional micro-slip is small compared to the macro-slip ($s_\delta/s < 0.5\%$).

Figure 8 Micro-slip in the conformal and contraformal contact at the given reference condition (F_N = 3921 N, v_Σ = 8 m/s, s = 20% and ϑ = 90°C)

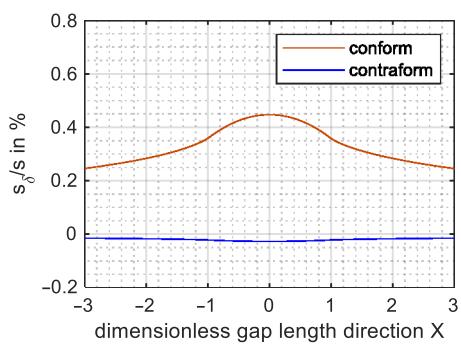

Source: Created by author

For an extended evaluation of the influence of the micro-slip, a greater range of slip values is considered. Also, different levels of conformity and equivalent radii of curvature are studied. For this purpose, a deformation of $\delta_{1,2}$ = 30 µm is assumed in equation (15), which corresponds to the maximum deformation for conformal contact at the reference operating condition (section 2.2) with a load of p_H = 1,200 N/mm^2. The level of conformity *loc* is defined as:

$$loc = \frac{R_1 - R_2}{R_1 + R_2}. \tag{16}$$

In general, *loc* increases for increasing conformity between two rolling elements. In case of $R_1 = R_2$ as strict contraformal contact, *loc* is zero. For $R_1 = \infty$ corresponding to a contact of a disk and plane, *loc* is 1. The conformal contact given in Figure 2 corresponds to *loc* = 1.94. Conformal contacts show values of *loc* > 1. For journal bearings, *loc* tends toward infinity.

Figure 9 shows the influence of the micro-slip related to the macro-slip for the conformal contact (brown line). Furthermore, the influence of varying *loc* (a) and R_x (b) on the relative micro-slip is shown. It can be seen that the influence of the micro-slip becomes strong for very low slip values, high *loc* (a) and low radii of curvature R_x (b). In detail, this occurs at high ratios between the deformation (δ) and the macroscopic radius of curvature "R", which occurs for high pressures and rolling elements with small dimensions.

As the micro-slip has only noticeable influence for small slip values, the investigation of the influence of the micro-slip on the coefficient of friction is focused on low slip values at the reference operating condition. Figure 10 shows the calculated friction curves for the conformal disk contact with ($s_\delta + s$) and without (s) considering micro-slip. Especially for very small macro-slip, a larger influence of the micro-slip is recognizable. With increasing macro-slip, the influence of micro-slip diminishes rapidly.

3.3 Scale effect

The results in sections 3.1 and 3.2 show that local contact effects like contact curvature and micro-slip have an influence on the coefficient of friction of the conformal contact. However, for hard EHL contacts with noticeable slip values, these influences become neglectable. Therefore, the contraformal and conformal hard EHL contact mainly differ in the equivalent radius of curvature. Considering this scale effect,

Figure 9 Influence of *loc* (a) and R_x (b) on the relative micro-slip s_δ

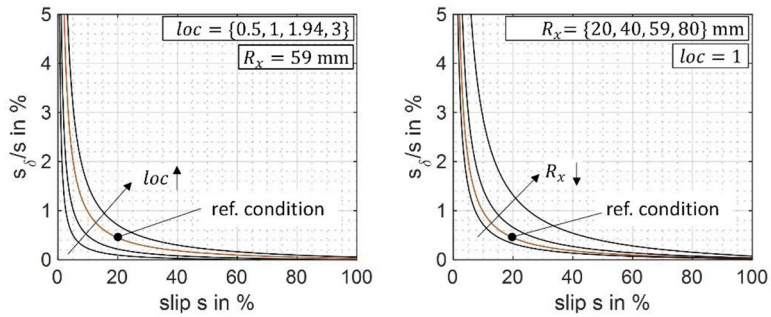

Source: Created by author

Figure 10 Influence of considering micro-slip on the coefficient of friction for the conformal contact

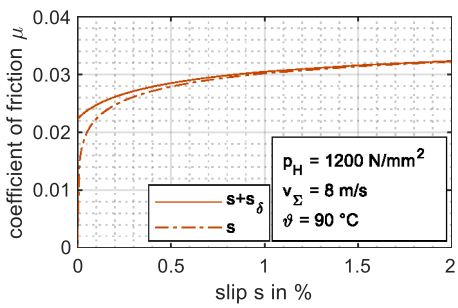

Source: Created by author

the influence of the equivalent radius of curvature is investigated for the considered conformal and contraformal disk contact (Figure 2) both for the same normal force F_N and the same nominal Hertzian pressure p_H. Figure 11 shows the calculated film thickness and contact temperature distribution as well as the derived fluid coefficient of friction μ for the equivalent radius of curvature R_x = 20 mm corresponding to the contraformal disk contact and R_x = 59 mm corresponding to the conformal disk contact. The conformal disk contact shows for both, same normal force and same Hertzian pressure higher central (h_c) and minimum film thickness (h_m) compared to the contraformal disk contact. This is due to the higher conformity with greater contact inlet radius. The fluid coefficient of friction μ is lower for the conformal contact. For equivalent F_N, the contact pressure is lower due to the greater flattened area resulting in lower shear stress and μ. For equivalent p_H, the higher temperature rise, lower contact viscosity and shear stress results in lower μ.

Since the radius of curvature R_x strongly varies along the path of contact of internal gearings, the influence of varying equivalent radius of curvature R_x is studied. Figure 12 shows a variation of the radius of curvature R_x for equivalent F_N and equivalent p_H considering the influence on film thickness, contact temperature distribution and fluid coefficient of friction.

In case of equivalent p_H in Figure 12 (b), the film thickness h increases degressively with increasing equivalent radius of curvature R_x. Although the temperature gradient along the gap length direction is lower for high R_x, the maximum temperature rise ΔT increases with increasing R_x. This decreases the effective contact viscosity and, hence, the lubricant shear stress. Consequently, the coefficient of friction μ is lower for high R_x, but the dependency of μ on R_x gets less for higher R_x.

In case of equivalent F_N in Figure 12 (c), the contact pressure reduces with increasing R_x. The film thickness and the flattened area also increase with higher R_x. The temperature gradient along the gap length direction is higher for smaller R_x and reaches higher maxima. However, the resulting coefficient of friction decreases for increasing R_x, which is due to the lower pressure and consequently lower effective contact viscosity and shear stress.

4. Conclusion

In this study, a conformal hard EHL line contact as it occurs in internal steel gearings was studied using a numerical EHL model. The effects and relevance of contact geometry and local kinematics as well of scaling were investigated and classified to a contraformal hard EHL line contact for same normal force and same contact pressure. The conclusions can be summarized as follows:

- Conformal hard EHL contacts show a curved centerline due to the different radii of curvature of the rolling elements. This local contact conformity is small and can be estimated analytically.
- The local contact geometry introduces a friction force due to the asymmetrical contact pressure distribution. With increasing contact pressure, the influence on the overall coefficient of friction vanishes.
- Conformal hard EHL contacts show micro-slip depending on the deformation, distance of contact point and center of rotation. Also, a contraformal contact shows micro-slip if a macro-slip is imposed. While for the conformal contact the micro-slip is additional to the macro-slip, it is subtractive for the contraformal contact.
- The relevance of local contact conformity and micro-slip in conformal hard EHL contacts is small. Nevertheless, for internal gear contacts the effect of micro-slip has to be considered at the area of the pitch point, whereas the influence of the curvature increases for pressures relatively lower than the reference condition at 1.2 GPa.

Figure 11 Film thickness and temperature distribution for the considered conformal (a) and contraformal (b),(c) disk contact for v_Σ = 8 m/s, s = 20% and ϑ = 90°C considering same F_N = 3,921 N and p_H = 1,200 N/mm^2

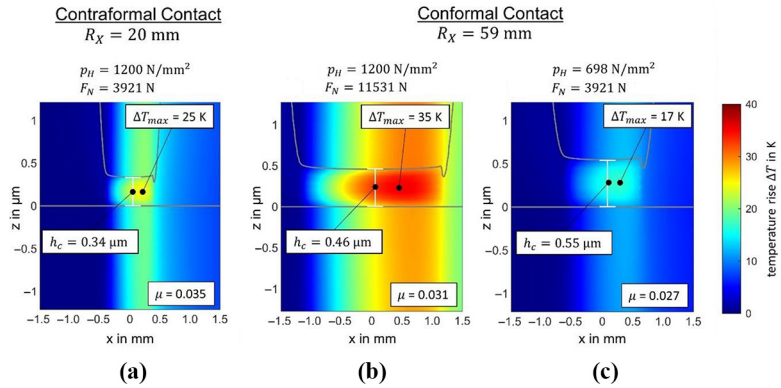

Source: Created by author

Figure 12 Influence of the equivalent radius of curvature R_x on the film thickness (a) and (b), maximum contact temperature (c) and (d) and fluid coefficient of friction (e) and (f) on the conformal disk contact for equivalent p_H = 1,200 N/mm^2 (a), (c) and (e), and equivalent F_N = 3,921 N (b), (d) and (f) for v_Σ = 8 m/s, s = 20% and ϑ = 90°C

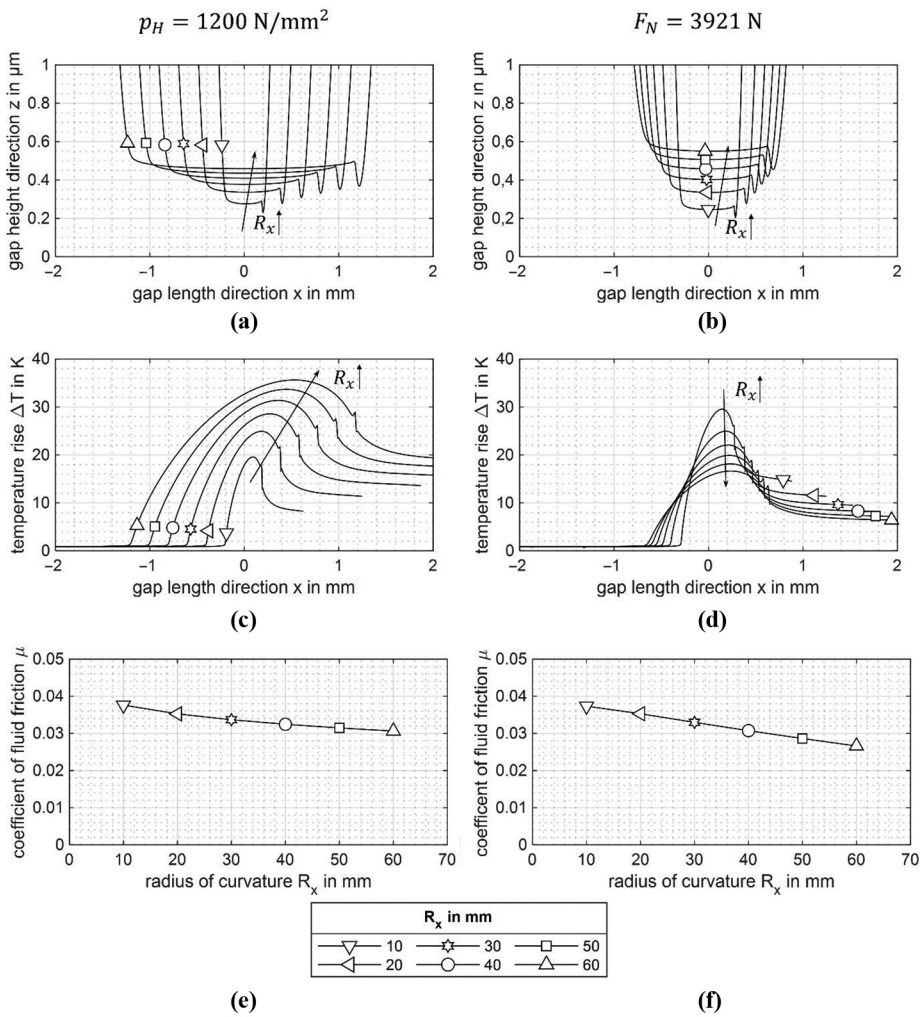

Source: Created by author

- Considering scale effects, the coefficient of friction decreases with increasing equivalent radius of curvature. For equivalent contact pressure, this is due to contact temperature rise. In case of equivalent normal force, it is due to the lower contact pressure.

As shown for hard conformal EHL contacts, the contact geometry and local kinematics can influence the contact conditions. It can be more strongly pronounced for softer EHL contacts e.g. with thermoplastics, on which further studies can be focused on.

References

Bartel, D. (2010), "Simulation von tribosystemen: Grundlagen und Anwendungen", Zugl.: Magdeburg, Univ., Fak. für Maschinenbau, Habil.-Schr., 2009, Wissenschaft, 1. Aufl., Vieweg + Teubner, Wiesbaden.

Bergmann, P., Grün, F., Grün, F., Gódor, I., Stadler, G. and Maier-Kiener, V. (2018), "On the modelling of mixed lubrication of conformal contacts", *In: Tribology International*, Vol. 125, pp. 220-236.

Blanco-Lorenzo, J., Santamaria, J., Vadillo, E.G. and Correa, N. (2018), "A contact mechanics study of 3D frictional conformal contact", *Tribology International*, Vol. 119, pp. 143-156.

Bobach, L. (2018), "Simulation dynamisch belasteter radiagleitlager unter mischreibungsbedingungen", Dissertation, Otto-von-Guericke-Universität Magdeburg.

Bode, B. (1989), "Modell zur Beschreibung des Fließverhaltens von Flüssigkeiten unter hohem Druck", *Tribologie Und Schmierungstechnik*, Vol. 36, pp. 182-189.

Booker, J.F., Boedo, S. and Bonneau, D. (2010), "Conformal elastohydrodynamic lubrication analysis for engine bearing design: a brief review", *Proceedings of the Institution of Mechanical Engineers, Part C: Journal of Mechanical Engineering Science*, Vol. 224 No. 12, pp. 2648-2653.

Czichos, H. and Habig, K.-H. (Eds) (2015), *Tribologie-Handbuch: Tribometrie, Tribomaterialien, Tribotechnik, 4., Vollst. überarb. und Erw. Aufl*, Springer Vieweg, Wiesbaden.

Eyring, H. (1936), "Viscosity, plasticity, and diffusion as examples of absolute reaction rates", *The Journal of Chemical Physics*, Vol. 4 No. 4, pp. 283-291.

Fagan, M.J. and McConnachie, J. (2001), "A review and detailed examination of non-layered conformal contact by finite element analysis", *The Journal of Strain Analysis for Engineering Design*, Vol. 36 No. 2, pp. 177-195.

Fang, N., Chang, L., Johnston, G.J., Webster, M.N. and Jackson, A. (1999), "An internal Line-Contact EHL and traction test rig", *International Fuels & Lubricants Meeting & Exposition*, OCT. 25, 1999, SAE International400 Commonwealth Drive, Warrendale, PA, United States (SAE Technical Paper Series).

Farrenkopf, F., Schwarz, A., Lohner, T. and Stahl, K. (2022), "Analysis of a Low-Loss gear geometry using a thermal elastohydrodynamic simulation including mixed lubrication", *Lubricants*, Vol. 10 No. 9, p. 200.

Fritzson, D. (2018), "Transient conformal TEHL algorithms for multibody simulation", *In: MIC*, Vol. 39 No. 3, pp. 209-232.

Fulcher, G.S. (1925), "analysis of recent measurements OF THE viscosity OF glasses", *Journal of the American Ceramic Society*, Vol. 8 No. 6, pp. 339-355.

Gevigney, J., Durand De; Ville, F., Changenet, C. and Velex, P. (2013), "Tooth friction losses in internal gears: analytical formulation and applications to planetary gears", *Proceedings of the Institution of Mechanical Engineers, Part J: Journal of Engineering Tribology*, Vol. 227 No. 5, pp. 476-485.

Habchi, W. (2018), *Finite Element Modeling of Elastohydrodynamic Lubrication Problems*, John Wiley & Sons, Hoboken, NJ, Chichester, UK.

Heathcote, H.L. (Ed.) (1921), "The ball bearing: in the making, under test and on service", *Proceedings of the Institution of Automobile Engineers*, Vol. 15 No. 1, pp. 569-702.

Hofmann, S., Yilmaz, M., Maier, E., Lohner, T. and Stahl, K. (2021), "Friction and contact temperature in dry rolling-sliding contacts with MoS2-bonded and a-C:H:Zr DLC coatings", *In: Int J Mech Mater Eng*, Vol. 16 No. 1.

Jia, H., Li, J., Wang, J., Xiang, G., Xiao, K. and Han, Y. (2019), "Micropitting fatigue wear simulation in Conformal-Contact Under mixed elastohydrodynamic lubrication", *Journal of Tribology*, Vol. 141 No. 6, p. 61501.

Johns-Rahnejat, P.M., Dolatabadi, N. and Rahnejat, H. (2020), "Analytical elastostatic contact mechanics of highly-loaded contacts of varying conformity", *Lubricants*, Vol. 8 No. 9, p. 89.

Johnson, K.L. (1970), "Regimes of elastohydrodynamic lubrication", *Journal of Mechanical Engineering Science*, Vol. 12 No. 1, pp. 9-16, doi: 10.1243/JMES_JOUR_1970_012_004_02.

Lang, O.R. and Steinhilper, W. (1978), *Gleitlager: Berechnung und Konstruktion von Gleitlagern mit konstanter und zeitlich veränderlicher Belastung; Mit 6 Arbeitsblättern, Konstruktionsbücher*, Vol. 31, Springer, Berlin.

Larsson, R. and Andersson, O. (2000), "Lubricant thermal conductivity and heat capacity under high pressure", *Journal of Engineering Tribology*, Vol. 214 No. 4, pp. 337-342.

Liu, X., Cui, J. and Yang, P. (2012), "Size effect on the behavior of thermal elastohydrodynamic lubrication of roller pairs", *Journal of Tribology*, Vol. 134 No. 1.

Liu, H.C., Zhang, B.B., Bader, N., Venner, C.H. and Poll, G. (2021), "Scale and contact geometry effects on friction in thermal EHL: twin-disc versus ball-on-disc", *Tribology International*, Vol. 154, p. 106694.

Lohner, T., Ziegltrum, A., Stemplinger, J.-P. and Stahl, K. (2016), "Engineering software solution for thermal elastohydrodynamic lubrication using multiphysics software", *Advances in Tribology*, Vol. 2016, pp. 1-13.

Maier, E., Ziegltrum, A., Lohner, T. and Stahl, K. (2017), "Characterization of EHL contacts of thermoplastic gears", *Forschung Im Ingenieurwesen*, Vol. 81 Nos 2/3, pp. 317-324.

Napel, W.E. (1994), "Elastohydrodynamics in counterformal and conformal contacts", *Applied Scientific Research*, Vol. 48 No. 2, pp. 159-173.

Philippon, D., Martinie, L. and Vergne, P. (2021), "Discussion on, scale and contact geometry effects on friction in thermal EHL: twin-disc versus ball-on-disc by liu, zhang, bader, venner, poll", *Tribology International*, Vol. 157, p. 106877.

Piccigallo, B. (1996), "A fast method for the numerical solution of thermal-elastohydrodynamic lubrication problems", *Wear*, Vol. 193 No. 1, pp. 56-65.

Roelands, C.J.A. (1966), "Correlation aspects of the viscosity-temperature relationship of lubricating oil", Dissertationsschrift Technische Hogeschool Delft.

Schleich, T. (2013), "Temperatur- und Verlustleistungsverhalten von Wälzlagern in Getrieben", Dissertation, Technische Universität München.

Schoo, A. (1985), "Verzahnungsverlustleistung in Planetenradgetrieben", Dissertation, Ruhr-Universität Bochum.

Schudy, J. (2010), "Untersuchungen zur Flankentragfähigkeit von Außen- und Innenverzahnungen", Dissertation, Technische Universität München, München.

Tammann, G. and Hesse, W. (1926), "Die Abhängigkeit der Viskosität von der Temperatur bei unterkühlten Flüssigkeiten", *Zeitschrift für anorganische und allgemeine Chemie*, Vol. 156 No. 1, pp. 245-257.

Vogel, H. (1921), "Das Temperaturabhängigkeitsgesetz der Viskosität von Flüssigkeiten", *Physik. Zeitschrift*, Vol. 22, pp. 645-647.

Zhang, M., Wang, J., Yang, P., Shang, Z., Liu, Y. and Dai, L. (2020), "A thermal EHL investigation for size effect of finite line contact on bush-pin hinge pairs in industrial chains", *Industrial Lubrication and Tribology*, Vol. 72 No. 5, pp. 695-701.

Ziegltrum, A., Lohner, T. and Stahl, K. (2017), "EHL simulation on the influence of lubricants on load-dependent gear losses", *Tribology International*, Vol. 113, pp. 252-261.

Ziegltrum, A., Lohner, T. and Stahl, K. (2018), "EHL simulation on the influence of lubricants on the frictional losses of DLC coated gears", lubricants", *Lubricants*, Vol. 6 No. 1, p. 17.

Corresponding author

Ferdinand Schmid can be contacted at: ferdinand.schmid@tum.de